

Denoising of Low Light Images using Patch Priors and Wavelets

Sreekala Kannothe, *Member, IAENG*, Sateesh Kumar H C, Raja K B

Abstract—The work aims to find a novel technique to remove noise from low light or low luminous level images to improve the visibility of the image and the performance of many image processing systems. A denoising technique using patch priors in wavelet domain for images with low luminous levels, with the help of the Gaussian Mixture Model, is presented here. The main idea is to perform denoising in a sparse domain. Initially, the image is decomposed into approximate and detailed components with the help of wavelet transform, and then the patch based Gaussian mixture model denoising process is applied on both approximate and detailed components. Expectation maximization algorithm is used for estimating the Gaussian mixture model parameters from the image patches. After denoising each component, inverse wavelet transform is applied to obtain the denoised output image. This denoising method was applied to a set of natural low luminous level images, and it resulted in clean images with good Peak Signal to Noise Ratio and Structural Similarity Index, compared to other conventional methods. This work is a novel method combining wavelet transform and Gaussian mixture model for the denoising of low light images.

Index Terms—EM algorithm, GMM, Denoising, MAP estimation, Wavelet decomposition.

I. INTRODUCTION

LOW Low light image processing has opened its wings to a wide range of applications, especially in the area of surveillance, and they include night surveillance through the usage of security cameras, target detection and recognition in defense, and health care through the new advent of medical imaging. The intensity of light is very feeble in such captured images, resulting in increased noise, resulting in poor visibility. Such images captured in low light environments affect the accuracy and performance of many image processing techniques. It is essential to enhance these images, and low light image enhancement is a relevant research topic among many researchers associated with image processing. However, the application of an enhancement scheme results in amplifying noise content too, which is undesired. There are many spatial domain [1] and transform domain [3], [12], [15] methods available in literature to reduce the noise level from images.

Discrete wavelet transform (DWT) decomposes a signal into two components, namely the coarse and the detailed, and performs the analysis at different frequency levels with

different resolutions. Coarse and detailed components are associated with low frequency and high frequency components, respectively. Successive highpass and lowpass filtering of the time domain signal results in these components. DWT finds many applications in signal and image processing areas, and one of the primary applications includes image denoising. In addition to DWT, there also exist other methods which use the wavelet thresholding technique for image denoising [11]. Compared to other multiscale representations, DWT helps in non-redundant restoration, giving better spatial and spectral localization of signal formation. Also, wavelet decomposition is very efficient in decoupling the higher order statistical features from images.

In this work, a patch based denoising in the wavelet domain is proposed for denoising low intensity images. Here the patches are modeled using Gaussian Mixture Model (GMM) in the wavelet domain. Gaussian distribution is well suited for modeling image patches and pixels [4]. Using GMM in the wavelet domain is similar to modeling the image patch with a constrained GMM. After performing noise removal for all the frequency bands, the inverse wavelet transform is applied to obtain a clear output image. A crisp survey of the articles referred to is described in section II, with the motivation and objectives of the proposed work being mentioned in section III, The methodology used in the implementation of the proposed research is explained in section IV and the simulation results are provided in section V. The conclusion is presented in section VI.

II. LITERATURE SURVEY

Lu-Jing Yi et al., [11] in their research work, have tried to remove the noise from the signal by making use of the threshold function in the wavelet domain. The authors have improvised the existing threshold function by incorporating what is known as adjustment factors. As per the authors, the wavelet threshold function depends primarily on selecting a proper threshold, which can be 'minimaxi', 'sqrtwolog', 'heursure', 'fixed', etc. In this research work, the authors have proposed an improved threshold based on the fixed threshold and then apply this for denoising various signals and then perform a comparative analysis. The authors, through their results, have validated that the proposed scheme of denoising has improved the signal-to-noise ratio by filtering the signals and reducing the mean square errors.

Wang Chunli et al., [5] in their work, have developed a denoising algorithm that works on speech signals. They have taken a noisy speech signal as the input and have initially converted that signal into the wavelet domain. In the wavelet domain, the authors have applied the wavelet threshold function, filtered the signal coefficients from the

Manuscript received September 10, 2020; revised August 02, 2021.
Sreekala K is a research scholar from Saphthagiri College of Engineering (Affiliated to VTU, Belagavi), Bengaluru. (corresponding author e-mail: kannothsree@gmail.com)
Sateesh Kumar H C is Professor and Head of Department, Electronics and Communication Engineering, Saphthagiri College of Engineering (Affiliated to VTU, Belagavi), Bengaluru.(e-mail: hcsateesh@yahoo.com)
Raja K B is Professor and Chairman, Department of Electronics and Communication Engineering, University Visvesvaraya College of Engineering, Bengaluru. (e-mail:raja_kb@yahoo.com)

noisy signal, and extracted the signal components that are then made to undergo an inverse wavelet transform, thus resulting in the denoised and reconstructed signal. In this paper, the authors have estimated the threshold using the steepest descent algorithm and several other adaptations. The authors have compared the threshold functions like hard threshold and soft threshold and, through their results, have established that the usage of hard threshold in wavelet domain may lead to an increase in discrete points, and usage of the soft threshold may result in increased loss of information.

The authors of [6] have proposed a new algorithm for noise removal in images by making use of wavelet transform and threshold function. The authors have mentioned that the signal transformation into the wavelet domain will result in the noise getting distributed over the entire time axis because of the non-wavelet coefficients. In contrast, the signal will get concentrated due to the lower number of coefficients in the wavelet domain. The denoising in the signals when performed using the threshold function depends on a comparison between the coefficients in the transformed domain and the threshold value, and these coefficients, which are processed, are then reconstructed to obtain a denoised signal.

The authors of [7] have used a hyperbolic tangent function for estimating the threshold function used for denoising in the wavelet domain. The objectives of their research work were to introduce a new threshold function in the wavelet domain that can be used for denoising applications. The authors have then optimized the shape parameters of the new threshold function by making use of the 'Artificial Fish Swarm' algorithm and through their results have shown that the denoising effect with this new threshold function based on hyperbolic tangent function and optimized in the shape parameter through the artificial fish swarm algorithm, is better than the traditional wavelet threshold function used in the wavelet domain. Their research has shown that using that threshold function will result in better continuity and maintainability to improve the denoising effect.

The combination of wavelet transform and singular vector decomposition is used for noise removal from a signal in work proposed in [8]. The author has compared and validated that the usage of this combination is better than using the wavelet transform alone when being used for noise removal from a signal. The deviation shown by the data points over a particular dimension can be ordered and identified by using a method called singular vector decomposition, which allows unearthing the most appropriate approximations for the data points, thus resulting in the reduction of noise and this when combined with the wavelet transform which has the advantage of representing the signal in time-frequency domain results in enhanced removal of noise.

Image denoising is a very critical requirement for low light image enhancement, and this is obvious from the literature available and Julie Delon et al., in their work [4] have proposed to denoise the image by making use of patch based priors using the Gaussian Mixture model. The authors reveal that the method involved in image denoising using the patch based method consists of several steps that include extracting patches from the input denoise image as the first step. The extracted patches are then grouped and modeled

using the Gaussian mixture model, and the estimation of the image parameters is then performed by using various estimation strategies like MAP (Maximum A Posteriori), MMSE (Minimum Mean Square Error), and linear MMSE. Finally, this method involves aggregating all the denoised patches to form a clean output image with a noise reduction.

There is considerable literature available about the techniques used for noise reduction in images used in medical and other applications where the presence of noise may result in contamination of results and usage of filters have helped in the reduction of the same [9], [10], [17]. They speak about noise reduction using filters like Gaussian filter, classic filter, and median filter and also have analyzed the performance of different filters in terms of noise reduction from medical images. Noise covariance is measured by using an adaptive Kalman filter which is constrained and unscented, and the design of the same has been stressed in [16]. Denoising of colour images has been implemented by using a norm minimization technique that is multi-channel weighted [18], and the authors have used spatial filters initially, and the resultant images after filtering are then used as input to their sequential algorithm, and hence they have named their method as having a warm start.

III. MOTIVATION AND OBJECTIVE

From the literature reviewed, it is seen that the denoising of images can be done in many ways, but there is a considerably good amount of research that performs image denoising by making use of wavelet threshold. However, as seen from [4], patch based denoising using GMM is also one of the better ways to achieve the same, and this proposed work aims at performing the denoising of low light images by using patch based method in the wavelet domain. The literature shows a void in the image denoising methods, which is done in sparse domain with the help of patch priors. The patch priors, when modelled with GMM and estimating the parameters by using any one of MAP, MMSE, or linear MMSE, is one such technique that is used in denoising a low light image. This work has identified the image denoising by using patches and modelling using GMM as its primary objective, and the method is discussed in detail in the below sections.

IV. METHODOLOGY

In this proposed patch based denoising method, noise removal is done in the wavelet domain using GMM. This is performed for all the frequency components of the input image. In this method, GMM parameters are found from patches using the Expectation-Maximization (EM) algorithm, and with the help of these parameters, patches are updated using Maximum A Posteriori (MAP) estimation. Then the denoised image is generated by aggregating the denoised patches. The parameter estimation and patch estimation happen periodically until a clear output image is obtained. Outline of the complete denoising process used here is given in figure (1).

Initially, the image is decomposed into low and high frequency components with the help of discrete wavelet transform. The low frequency part is the approximate component, and there are three high frequency components, namely

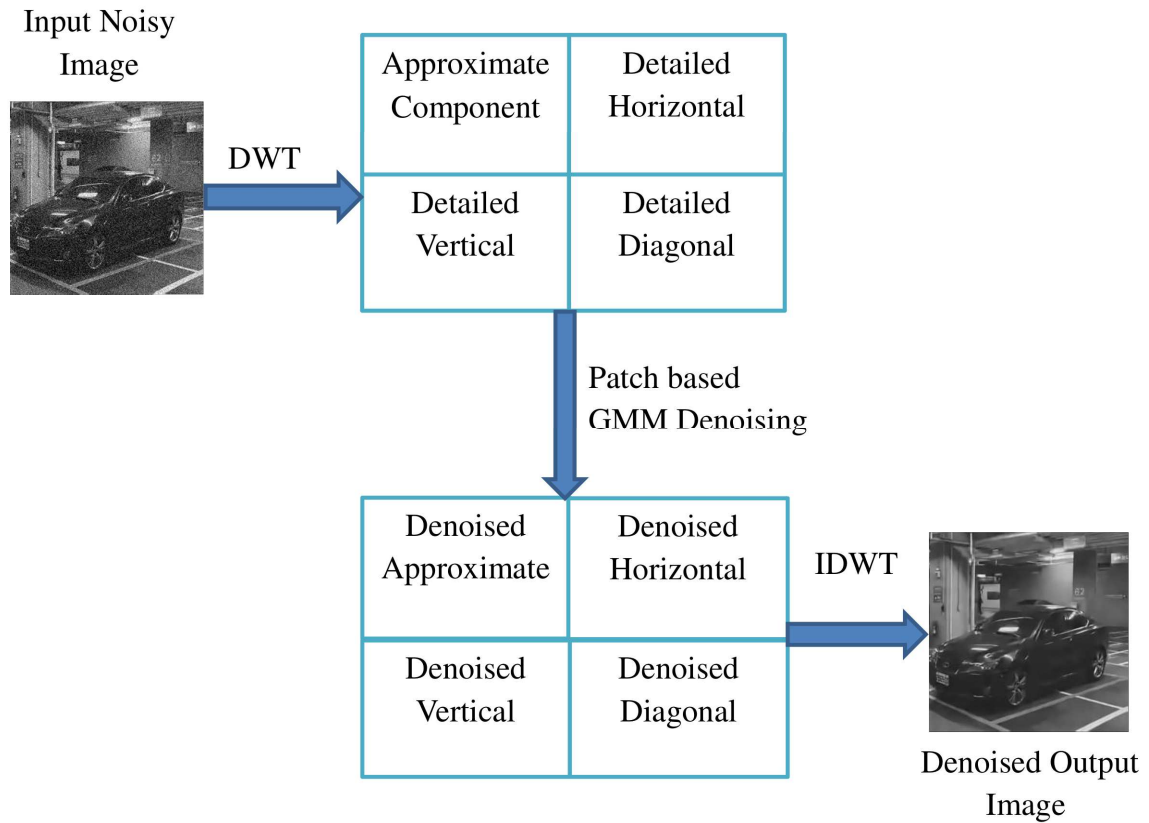


Fig. 1: Outline of the complete process

detailed horizontal, detailed vertical, and detailed diagonal components. After the wavelet decomposition, a patch based denoising technique using GMM is applied to all the low and high frequency components separately. In patch based denoising process using GMM, patches are extracted from the approximate component of the noisy input image in the initial step. The patches of the approximate component are grouped and modeled using GMM.

Model parameters are initialized by using the maximum log-likelihood function and Gaussian parameters to get the MAP estimation. The estimated image patches are then restored, and clean patches are aggregated to recover the denoised image components. Then the same process is performed for all three detailed components.

For the k_i^{th} model, MAP estimation for the i^{th} image patch \tilde{P}_i is given as

$$\tilde{P}_i = (\Sigma_{k_i} + \sigma^2 I)^{-1} (\Sigma_{k_i}^y + \sigma^2 \mu_{k_i}) \quad (1)$$

The estimation of the denoised image \tilde{x} from the patches is given as,

$$\tilde{x} = (\lambda I + \beta \sum_i R_i^T R_i)^{-1} (\lambda I y + \beta \sum_i R_i^T \tilde{P}_i) \quad (2)$$

where regularization parameters are represented by λ and β [2]. The window used in the extraction of the i^{th} patch is represented by R_i , the noisy component is represented by y , the identity matrix is represented by I .

Then EM algorithm is used to update GMM which in turn updates the patches. Steps involved in this process are:

- Calculate the likelihood of the fresh patch with the help of equation 3, [13] which is given as

$$\gamma_{ki} = \frac{\pi_k \mathcal{N}(\tilde{p}_i | \mu_k, \Sigma_k)}{\sum_{l=1}^K \pi_l \mathcal{N}(\tilde{p}_i | \mu_l, \Sigma_l)} \quad (3)$$

for $i = 1, 2 \dots n$ and $k = 1, 2 \dots K$

- Gaussian parameters are updated using a linear combination of new data and parameters (π_k, μ_k, Σ_k) , as shown in equations 4, 5 and 6 [13].

$$\tilde{\pi}_k = a_k \frac{n_k}{n} + (1 - a_k) \pi_k \quad (4)$$

$$\tilde{\mu}_k = a_k \frac{1}{n_k} \sum_{i=1}^n \gamma_{ki} \tilde{P}_i + (1 - a_k) \mu_k \quad (5)$$

$$\begin{aligned} \tilde{\Sigma}_k = & a_k \frac{1}{n_k} \sum_{i=1}^n \gamma_{ki} (\tilde{P}_i - \tilde{\mu}_k) (\tilde{P}_i - \tilde{\mu}_k)^T \\ & + (1 - a_k) (\Sigma_k + (\mu_k - \tilde{\mu}_k) (\mu_k - \tilde{\mu}_k)^T) \end{aligned} \quad (6)$$

Restoring the image patches using MAP estimation and updating Gaussian parameters are performed periodically until an image with a satisfactory noise level is obtained. The resulting denoised image component is the denoised approximate component. The above process is applied on detailed horizontal, vertical, and diagonal components separately to obtain their denoised versions. Finally, performing the inverse discrete wavelet transform results in the formation of a clear denoised image. In the end, results are compared

with the help of Peak Signal to Noise Ratio (PSNR) and Structural Similarity Index (SSIM).

V. SIMULATION RESULTS

Simulations were carried out on Plane, and Tiger images from Berkeley segmentation database [14]. Simulation was done by keeping noise level $\sigma = 5, 10, 15, 20, 30, 40, 50, 70$ and 100. Output images were observed in each case. Haar wavelet was used for decomposing image into low and high frequency components, and the patch size in the simulation was set to 8×8 . Figure (2) shows the noisy images of Plane and Tiger with noise level $\sigma = 20$. Figure (3) and figure (4) are the results of decomposition using Haar wavelet on noisy Plane and Tiger images, respectively, and the result of denoising on the decomposed components. It is seen from the decomposed noisy and denoised components that the level of noise is considerably reduced in the transform domain with the help of the proposed method. The final reconstructed output is obtained by applying inverse wavelet transform on the denoised components. Simulation output on the above two images with noise level $\sigma = 20$, using the proposed method along with the result of conventional wavelet thresholding technique is shown in figure (5) and figure (6).

Peak signal to noise ratio (PSNR) and structural similarity index (SSIM) values were also calculated for the noisy image and noise-free images, and they are tabulated for the noise level $\sigma = 5, 10, 15, 20, 30, 40, 50, 70$ and 100. Table (I) gives the PSNR values, and table (II) gives the SSIM values obtained from the proposed method for the two images along with the corresponding PSNR and SSIM values obtained using the wavelet thresholding technique. From the values shown in table (I), it is evident that the PSNR values of the proposed denoising method are higher than the PSNR values of the denoising techniques based on the conventional wavelet thresholding technique. PSNR is an image quality metric that is used to measure the performance of any image processing algorithm, and it gives the ratio of the peak value of the signal to the noise level in the signal and thus higher the value of PSNR suggests a better signal strength compared to the one with lower PSNR value. The PSNR values of the noisy images are also provided in the table, which is very low compared to the PSNR values of the denoised images using the proposed method. This can be further explained by taking one of the noise levels, say $\sigma = 20$. For this value of the noise level, the PSNR value of the noisy input image is 22.1874dB, and the PSNR values of the denoised images using conventional wavelet thresholding technique and the proposed denoising technique are 26.0290dB and 29.7530dB, respectively, which allows us to draw the inference that the proposed method has a better PSNR value which shows that it performs better in image denoising compared to the conventional denoising method in the wavelet domain. This is true not just for the noise level of $\sigma = 20$, but also for other noise levels for which the values have been provided in the table, thus leading to a conclusion that the PSNR values of the proposed denoising method are very much higher compared to that of the noisy input image and the denoised images using conventional wavelet thresholding technique. Thus, the proposed method is more efficient than denoising based on the conventional wavelet thresholding technique in removing noise from a noisy input image.

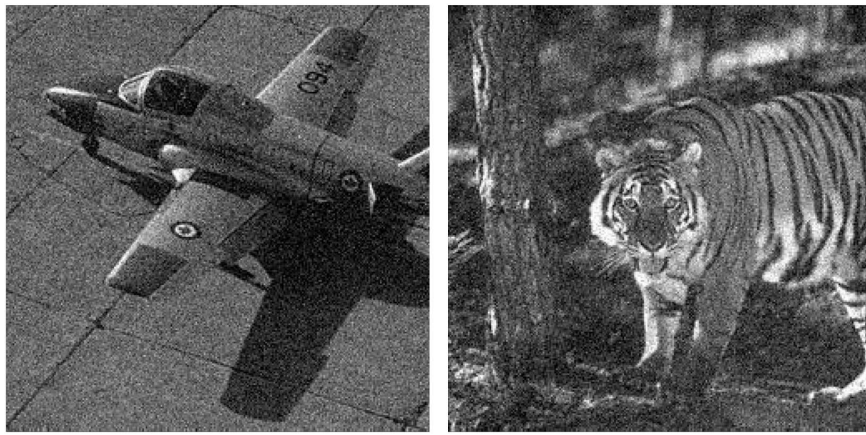
The other quality metric used in this proposed work to evaluate the performance is the structural similarity index measure (SSIM) which highlights the similarity in the structure of the image when compared with the ground truth. The SSIM values for various noise levels have been tabulated in table (II). Similar to the case of PSNR, let us take the case of noise level $\sigma = 20$. For this noise level, it is observed that the value of SSIM for the noisy input image is 0.3468, whereas the SSIM value of the conventional wavelet thresholding technique based denoising method is observed to be 0.5217 and that of the proposed denoising method is 0.7968. This indicates that the denoised image obtained with the proposed method is having a similarity of 79.68% to the ground truth image when compared to that of 52.17% that is obtained with the conventional wavelet thresholding technique based denoising method and 34.68% that is of the noisy input image. These values further consolidate that our proposed denoising method provides a better output not just in terms of the increased signal values but also in terms of increased similarity with the ground truth images. The SSIM values show a consistent value for all the noise levels as shown in the table (II) and not just for the noise level of $\sigma = 20$. This enables us to conclude that the proposed method is more

TABLE I: Quality metrics - PSNR values

Image	Noise Level(σ)	Noisy Image	Wavelet threshold	Proposed Method
Plane	5	34.1320	35.8288	37.3635
	10	28.1550	31.1768	33.4833
	15	24.6651	28.2531	31.1848
	20	22.1874	26.0290	29.7530
	30	18.8314	22.7607	28.1549
	40	16.4644	20.4698	27.1690
	50	14.7182	18.7556	26.3778
	70	12.3022	16.0624	25.2685
Tiger	5	34.0979	33.5822	35.9668
	10	28.0978	30.1093	31.3778
	15	24.6491	27.4843	28.9309
	20	22.2134	25.4743	27.3515
	30	18.7499	22.4476	25.3791
	40	16.4610	20.2619	24.0335
	50	14.7955	18.5674	23.2029
	70	12.4288	15.9550	21.8778
100	10.3005	13.4498	20.8219	

TABLE II: Quality metrics - SSIM values

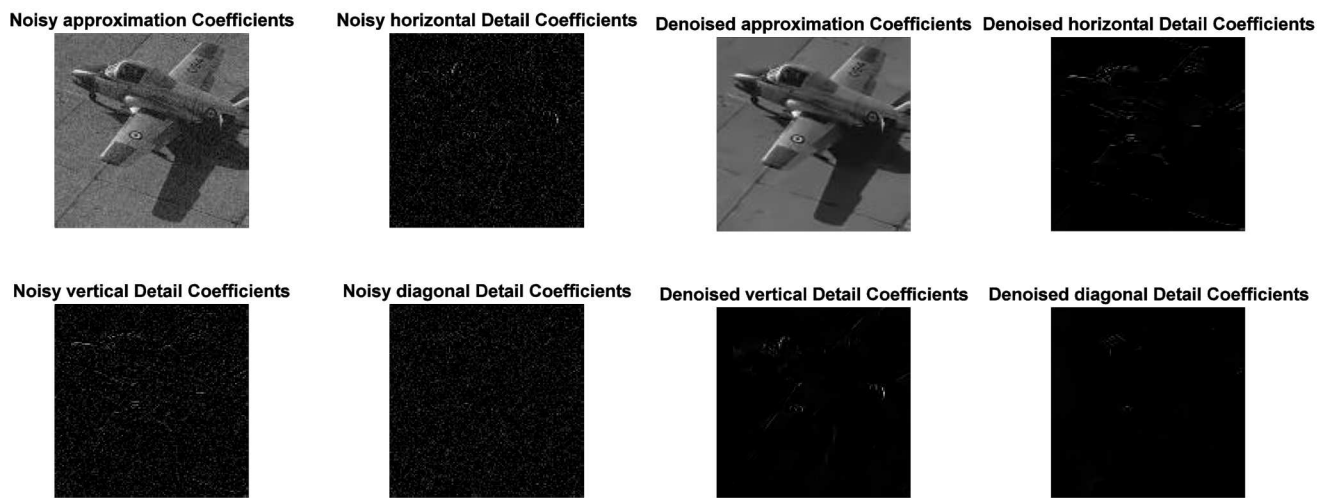
Image	Noise Level(σ)	Noisy Image	Wavelet threshold	Proposed Method
Plane	5	0.8420	0.9098	0.9328
	10	0.6117	0.7681	0.8789
	15	0.4505	0.6335	0.8341
	20	0.3468	0.5217	0.7968
	30	0.2279	0.3650	0.7382
	40	0.1649	0.2742	0.6996
	50	0.1227	0.2191	0.6624
	70	0.0793	0.1450	0.5979
Tiger	5	0.9288	0.9401	0.9599
	10	0.7898	0.8733	0.9018
	15	0.6633	0.7876	0.8468
	20	0.5613	0.7068	0.7987
	30	0.4088	0.5645	0.7207
	40	0.3130	0.4632	0.6542
	50	0.2499	0.3874	0.6056
	70	0.1702	0.2810	0.5216
100	0.1087	0.1889	0.4470	



(a). Noisy Plane Image

(b). Noisy Tiger Image

Fig. 2: Noisy input Images - Plane and Tiger



(a). Decomposed noisy components

(b). Decomposed dnoised components

Fig. 3: Decomposed noisy components and its denoised versions - Plane image

efficient in removing noise by increasing the signal level in the image and maintaining the structural similarity of the output image with the ground truth image. A plot of these values against σ is shown in figure (7) and figure (8). The graph shows that the proposed method using wavelet has better PSNR and SSIM values than the conventional wavelet thresholding method. This means that the proposed method is efficient in removing the noise component by keeping the signal level high, retaining the edges and structure of the image.

The proposed denoising technique is applied to natural images with low luminous levels from the data set created. This data set contains images captured at different luminous levels for simulation purposes. Images of Car, Cup, Building, and Sculpture captured at different luminous levels, and with the noise level of $\sigma = 5, 10, 20, 30, 40, 50, 70, 100$ were considered for simulation. Simulation results for one set of luminous level images are shown in figure (9), figure (10) and figure (11). Table (III) to Table (VI) shows the Quality metrics (SSIM and PSNR) values for the images with different luminous level and varying noise levels.

Figure (12) to figure (19) shows the graph of PSNR and SSIM values plotted against noise levels (σ) for different light intensity images of Car, Cup, Building and Sculpture. The light intensity level at which the images are captured is given in the corresponding graph. Figure (12) and figure (13) are the plots of PSNR and SSIM values for Car images of intensities 315, 282, 261, 232 against noise levels 5, 10, 20, 30, 40, 50, 70, 100. Figure (14) and figure (15) are the same plots for Cup images of intensities 98, 72, 61, 49 against noise levels 5, 10, 20, 30, 40, 50, 70, 100. Figure (16) and figure (17) are the plots of PSNR and SSIM values for Building images of intensities 321, 298, 253, 230 against the same noise levels 5, 10, 20, 30, 40, 50, 70, 100. Finally figure (18) and figure (19) are the plots of PSNR and SSIM values for Sculpture images of intensities 152, 140, 112, 84 against noise levels 5, 10, 20, 30, 40, 50, 70, 100. It is seen from the graph that the proposed method is effective in removing high noise levels, which resulted in comparatively high PSNR and SSIM values compared to noisy images. A plot of PSNR and SSIM against different intensity levels for the images are given in figure(20) for a single noise level of $\sigma = 20$.

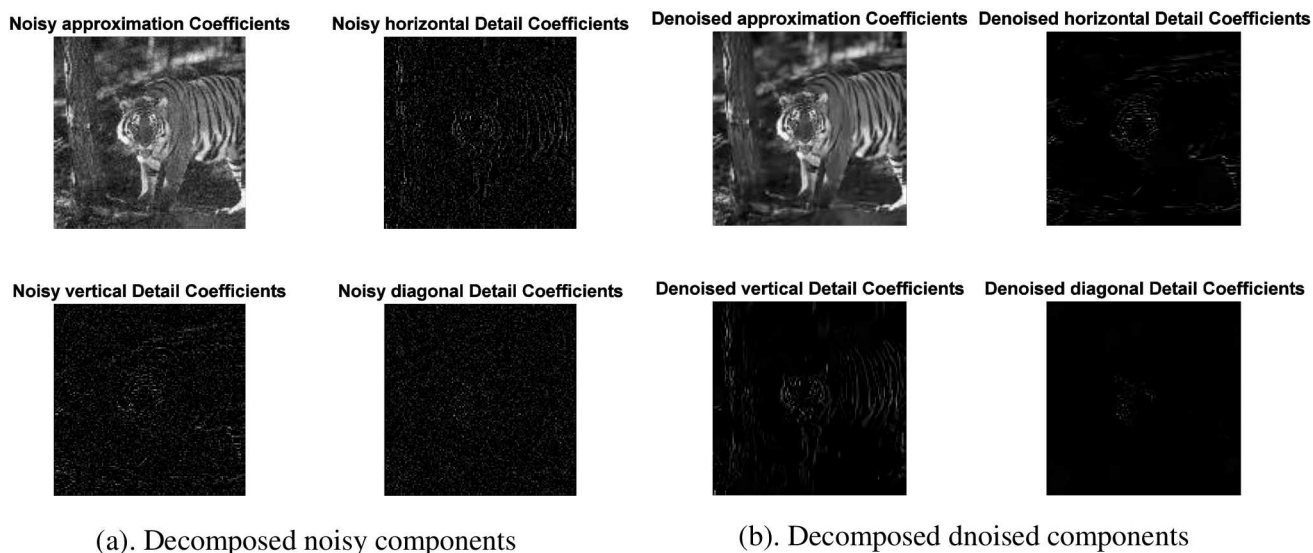


Fig. 4: Decomposed noisy components and its denoised versions - Tiger image

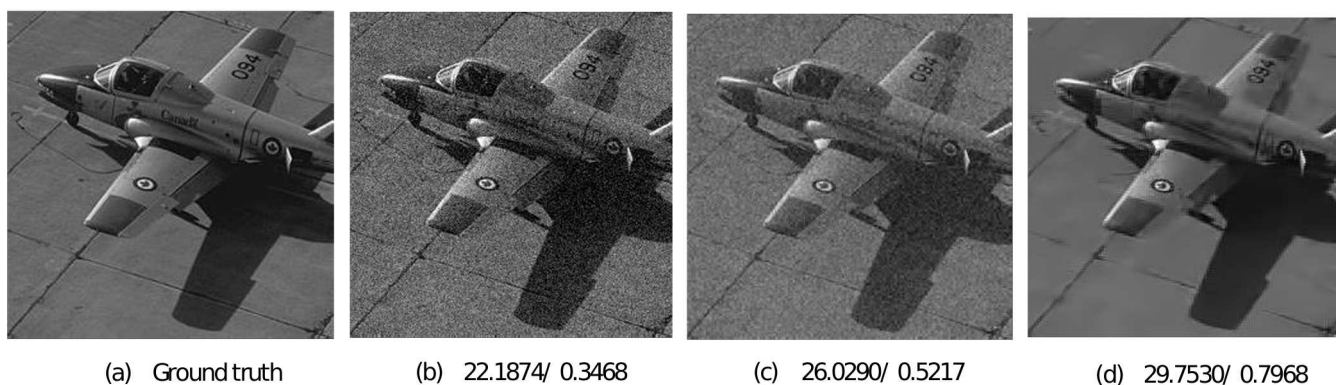


Fig. 5: Results of denoising on Plane image for noise level(σ) = 20 with PSNR/SSIM values below the image. (a) Ground truth (b) Input noisy Image (c) Result of denoising with conventional wavelet thresholding technique (d) Result of denoising using proposed technique

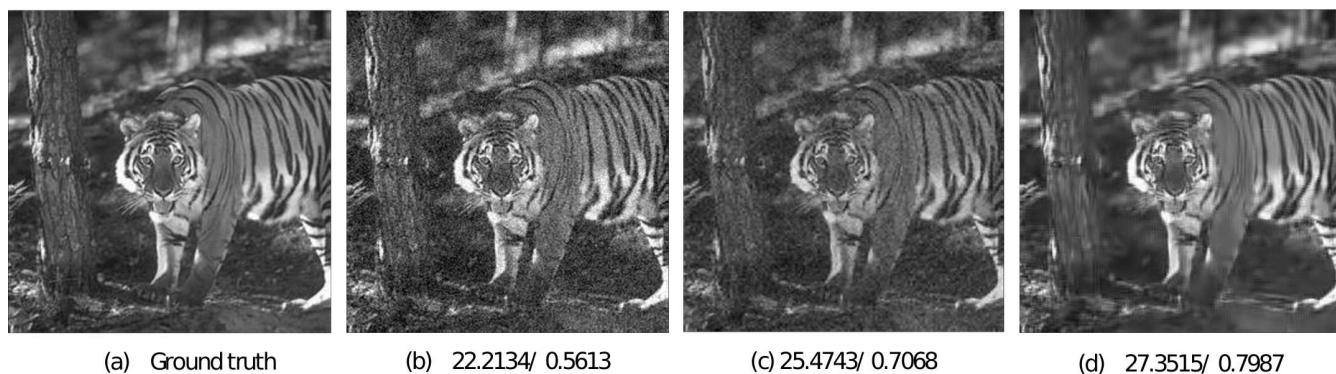


Fig. 6: Results of denoising on Tiger image for noise level(σ) = 20 with PSNR/SSIM values below the image. (a) Ground truth (b) Input noisy image (c) Result of denoising with conventional wavelet thresholding technique (d) Result of denoising using proposed technique

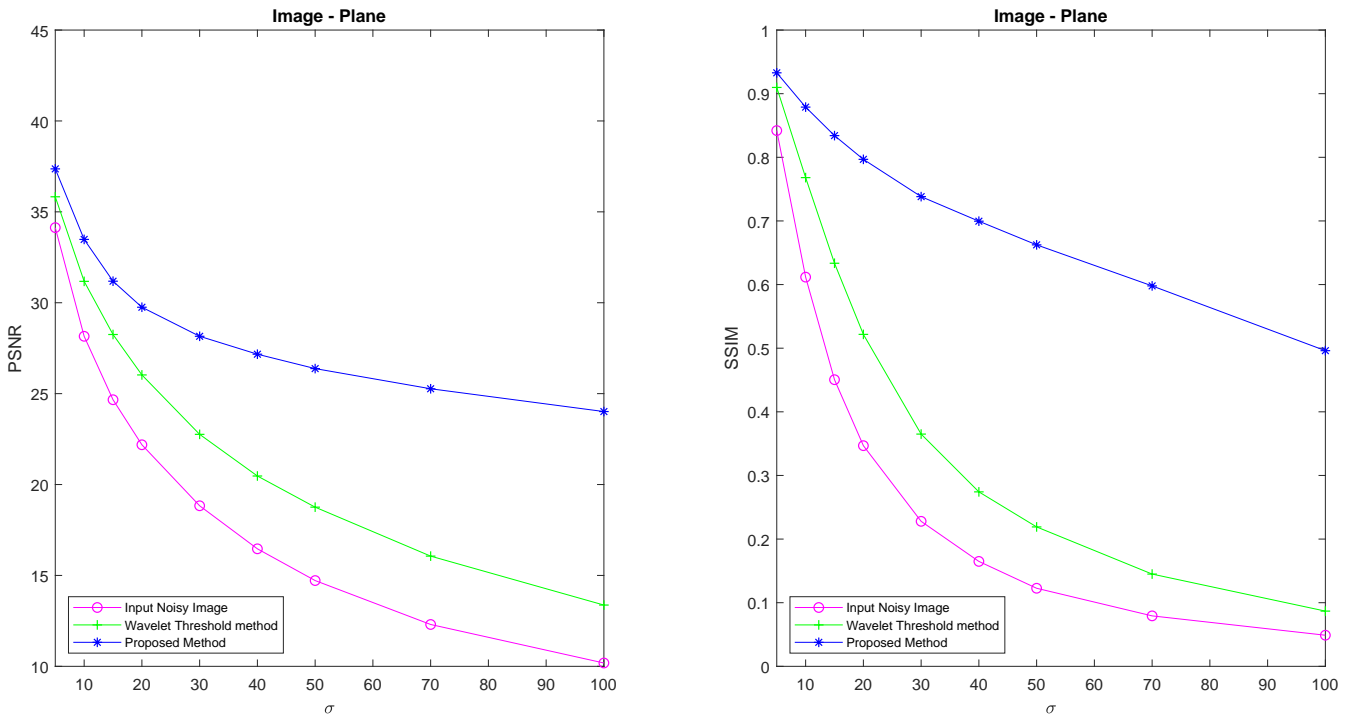


Fig. 7: Plot of quality metrics values for Plane images against varying noise levels.

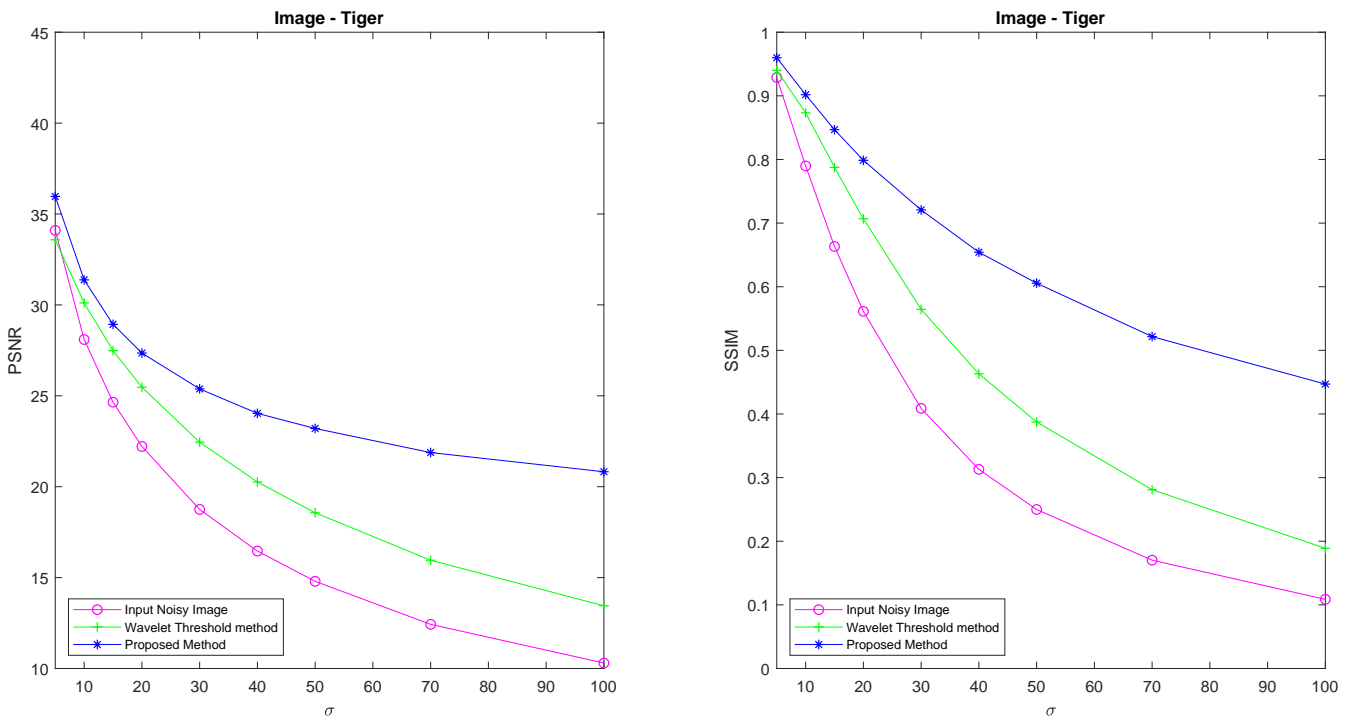


Fig. 8: Plot of quality metrics values for Tiger images against varying noise levels.



Fig. 9: Ground truth of natural low luminous level images used for simulation
These sample images are captured at light intensities: Car - 315 lux, Cup - 98 lux,
Building - 321 lux and Sculpture - 152 lux.

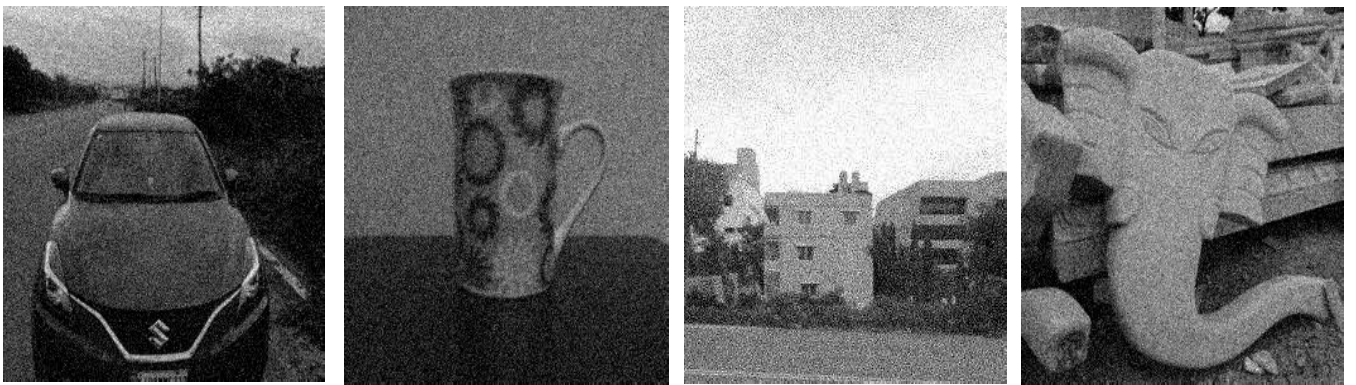


Fig. 10: Noisy versions of the ground truths, with noise level $\sigma = 20$



Fig. 11: Result of denoising by proposed method on natural low luminous level images

TABLE III: Quality metrics for Car image with different noise levels and luminous levels

Image	Light Intensity	Noise level - σ	PSNR - Noisy Image	PSNR - Denoised Image	SSIM - Noisy Image	SSIM - Denoised Image
Car	315	5	34.1923	37.6698	0.8599	0.9585
	282	5	34.1543	37.6692	0.8574	0.9578
	261	5	34.2295	37.8686	0.8542	0.9574
	232	5	34.3746	38.1809	0.8446	0.9536
	315	10	28.2468	33.2415	0.6560	0.9082
	282	10	28.1167	33.2475	0.6463	0.9064
	261	10	28.2701	33.3971	0.6424	0.9036
	232	10	28.5267	33.9375	0.6268	0.9014
	315	20	22.2650	29.7803	0.4002	0.8282
	282	20	22.3172	29.6484	0.3981	0.8269
	261	20	22.5080	29.9583	0.3939	0.8254
	232	20	22.7104	30.5156	0.3717	0.8300
	315	30	18.9504	28.0071	0.2757	0.7731
	282	30	19.0711	28.0011	0.2761	0.7666
	261	30	19.1636	28.1268	0.2666	0.7652
	232	30	19.3754	28.7200	0.2483	0.7755
	315	40	16.6298	26.9855	0.2042	0.7282
	282	40	16.7707	26.7546	0.2022	0.7226
	261	40	16.9040	27.0339	0.1948	0.7240
	232	40	17.1065	27.5994	0.1814	0.7336
	315	50	14.8443	26.0172	0.1562	0.6883
	282	50	15.0643	26.0395	0.1572	0.6830
	261	50	15.1826	26.1062	0.1496	0.6782
	232	50	15.3996	26.6666	0.1398	0.6898
	315	70	12.4694	24.9831	0.1027	0.6343
	282	70	12.6199	24.9206	0.1038	0.6091
	261	70	12.8077	25.0518	0.0997	0.6106
	232	70	12.9247	25.2872	0.0885	0.6183
	315	100	10.3195	23.6403	0.0656	0.5460
	282	100	10.3753	23.6041	0.0624	0.5371
261	100	10.5015	23.7110	0.0601	0.5261	
232	100	10.5529	24.0447	0.0534	0.5178	

TABLE IV: Quality metrics for Cup image with different noise levels and luminous levels

Image	Light Intensity	Noise level - σ	PSNR - Noisy Image	PSNR - Denoised Image	SSIM - Noisy Image	SSIM - Denoised Image
Cup	98	5	34.1613	41.7073	0.7698	0.9653
	72	5	34.2178	41.7488	0.7705	0.9653
	61	5	34.8800	42.2692	0.7622	0.9627
	49	5	35.1222	43.0420	0.7086	0.9679
	98	10	28.1197	39.1145	0.4796	0.9512
	72	10	28.3524	39.0500	0.4911	0.9496
	61	10	28.9743	39.3821	0.4755	0.9405
	49	10	29.1133	40.3471	0.4043	0.9488
	98	20	22.2786	35.7542	0.2202	0.9122
	72	20	22.7069	36.2031	0.2343	0.9160
	61	20	23.0716	36.7258	0.2094	0.9084
	49	20	23.2082	37.5624	0.1646	0.9022
	98	30	19.0172	34.2874	0.1281	0.8810
	72	30	19.3512	34.3993	0.1342	0.8801
	61	30	19.6740	34.9523	0.1126	0.8697
	49	30	19.8625	35.7810	0.0871	0.8713
	98	40	16.6854	32.8863	0.0823	0.8424
	72	40	17.0487	33.2033	0.0870	0.8449
	61	40	17.3797	33.6209	0.0700	0.8243
	49	40	17.6868	34.1224	0.0561	0.7935
	98	50	14.9340	31.7855	0.0581	0.8031
	72	50	15.2956	32.0040	0.0607	0.8003
	61	50	15.6886	32.9058	0.0487	0.7998
	49	50	15.9593	33.2060	0.0399	0.7126
	98	70	12.4880	29.6078	0.0343	0.6937
	72	70	12.8191	30.3268	0.0340	0.7267
	61	70	13.1808	30.6661	0.0277	0.7002
	49	70	13.4157	31.7391	0.0223	0.6531
	98	100	10.2473	28.2667	0.0183	0.6208
	72	100	10.5093	28.1555	0.0182	0.6053
61	100	10.7171	28.8975	0.0148	0.5945	
49	100	10.7858	28.6419	0.0114	0.4969	

TABLE V: Quality metrics for Building image with different noise levels and luminous levels

Image	Light Intensity	Noise level - σ	PSNR - Noisy Image	PSNR - Denoised Image	SSIM - Noisy Image	SSIM - Denoised Image
Building	321	5	34.6119	39.8243	0.8371	0.9717
	298	5	34.1696	39.7352	0.8088	0.9713
	253	5	34.1823	39.7399	0.8049	0.9698
	230	5	34.3910	40.5193	0.7908	0.9693
	321	10	28.7014	35.7745	0.6111	0.9420
	298	10	28.2244	35.7015	0.5618	0.9393
	253	10	28.2815	35.8407	0.5573	0.9388
	230	10	28.4962	36.6399	0.5336	0.9385
	321	20	22.8322	32.4760	0.3459	0.8939
	298	20	22.5763	32.4617	0.3158	0.8911
	253	20	22.4110	32.5379	0.3050	0.8846
	230	20	22.5503	33.0683	0.2828	0.8852
	321	30	19.5768	30.7154	0.2252	0.8545
	298	30	19.3276	30.5144	0.2074	0.8460
	253	30	19.1350	30.4653	0.1979	0.8347
	230	30	19.0878	31.2929	0.1755	0.8420
	321	40	17.2483	29.3476	0.1581	0.8061
	298	40	17.1451	29.2551	0.1473	0.7973
	253	40	16.9570	29.4079	0.1428	0.7992
	230	40	16.8477	29.9420	0.1224	0.7922
	321	50	15.4836	28.4331	0.1175	0.7770
	298	50	15.4044	28.3310	0.1104	0.7575
	253	50	15.2662	28.4798	0.1057	0.7484
	230	50	15.1886	28.9548	0.0918	0.7511
	321	70	12.9816	27.1064	0.0734	0.7038
	298	70	12.9819	26.8940	0.0710	0.6753
	253	70	12.8589	26.9130	0.0663	0.6650
	230	70	12.7618	27.4283	0.0563	0.6679
321	100	10.5567	25.6529	0.0423	0.6204	
298	100	10.6232	25.6333	0.0423	0.5850	
253	100	10.5493	25.4945	0.0387	0.5610	
230	100	10.5260	26.1578	0.0329	0.5833	

TABLE VI: Quality metrics for Sculpture image with different noise levels and luminous levels

Image	Light Intensity	Noise level - σ	PSNR - Noisy Image	PSNR - Denoised Image	SSIM - Noisy Image	SSIM - Denoised Image
Sculpture	152	5	34.1659	37.1090	0.8687	0.9400
	140	5	34.2264	37.2183	0.8712	0.9408
	112	5	34.2470	37.3038	0.8629	0.9400
	84	5	34.4492	37.4565	0.8543	0.9412
	152	10	28.2014	33.3981	0.6662	0.8918
	140	10	28.2912	33.5076	0.6622	0.8929
	112	10	28.3288	33.4882	0.6586	0.8912
	84	10	28.4662	33.6988	0.6426	0.8917
	152	20	22.2790	30.1817	0.4037	0.8227
	140	20	22.3212	30.2025	0.3998	0.8214
	112	20	22.4339	30.1950	0.3961	0.8177
	84	20	22.5168	30.4655	0.3808	0.8216
	152	30	18.9865	28.4358	0.2627	0.7661
	140	30	18.9165	28.4761	0.2665	0.7665
	112	30	18.9850	28.4684	0.2631	0.7651
	84	30	19.1030	28.7583	0.2490	0.7640
	152	40	16.4926	27.3959	0.1938	0.7303
	140	40	16.5256	27.2743	0.1921	0.7192
	112	40	16.5807	27.3829	0.1869	0.7151
	84	40	16.7319	27.5051	0.1772	0.7067
	152	50	14.6446	26.3542	0.1420	0.6794
	140	50	14.7438	26.4935	0.1434	0.6820
	112	50	14.8419	26.5525	0.1416	0.6855
	84	50	14.9674	26.7791	0.1295	0.6708
	152	70	12.2611	25.2818	0.0902	0.6228
	140	70	12.2817	25.2422	0.0905	0.6172
	112	70	12.3463	25.2524	0.0881	0.6140
	84	70	12.5423	25.4394	0.0825	0.5936
	152	100	10.1501	23.8239	0.0556	0.5394
	140	100	10.1693	23.6900	0.0535	0.5109
	112	100	10.2135	23.7657	0.0513	0.5205
	84	100	10.2847	24.0498	0.0478	0.4974

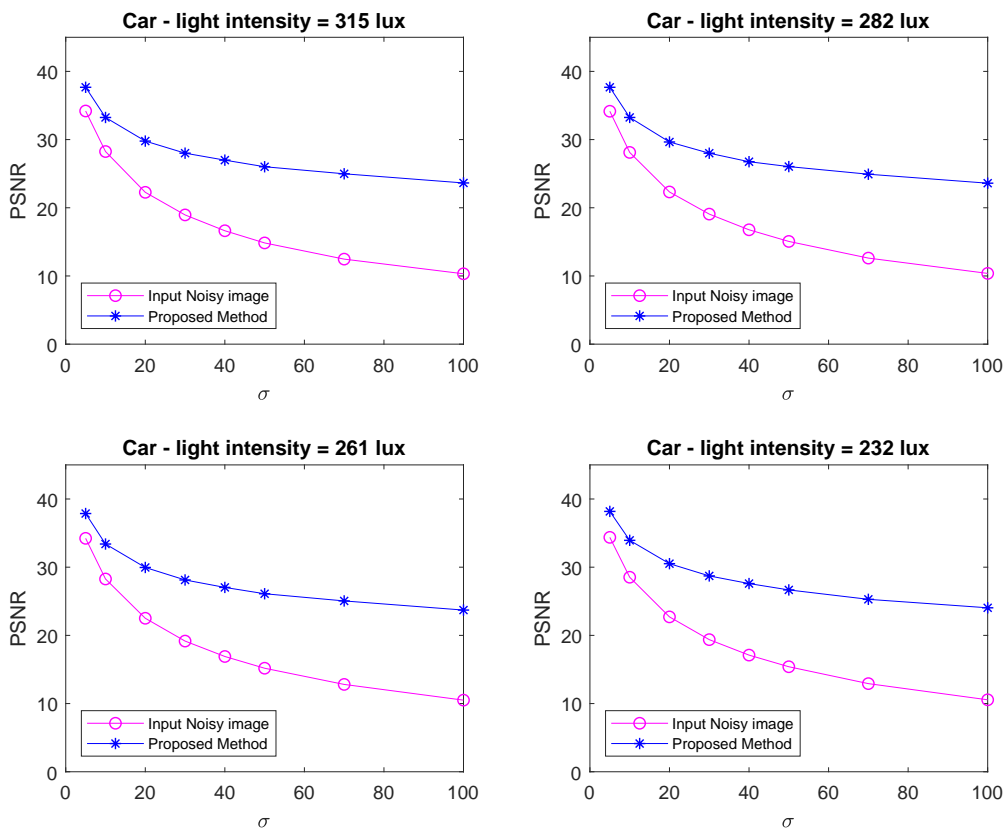


Fig. 12: Plot of PSNR values for Car images of different intensities against varying noise levels.

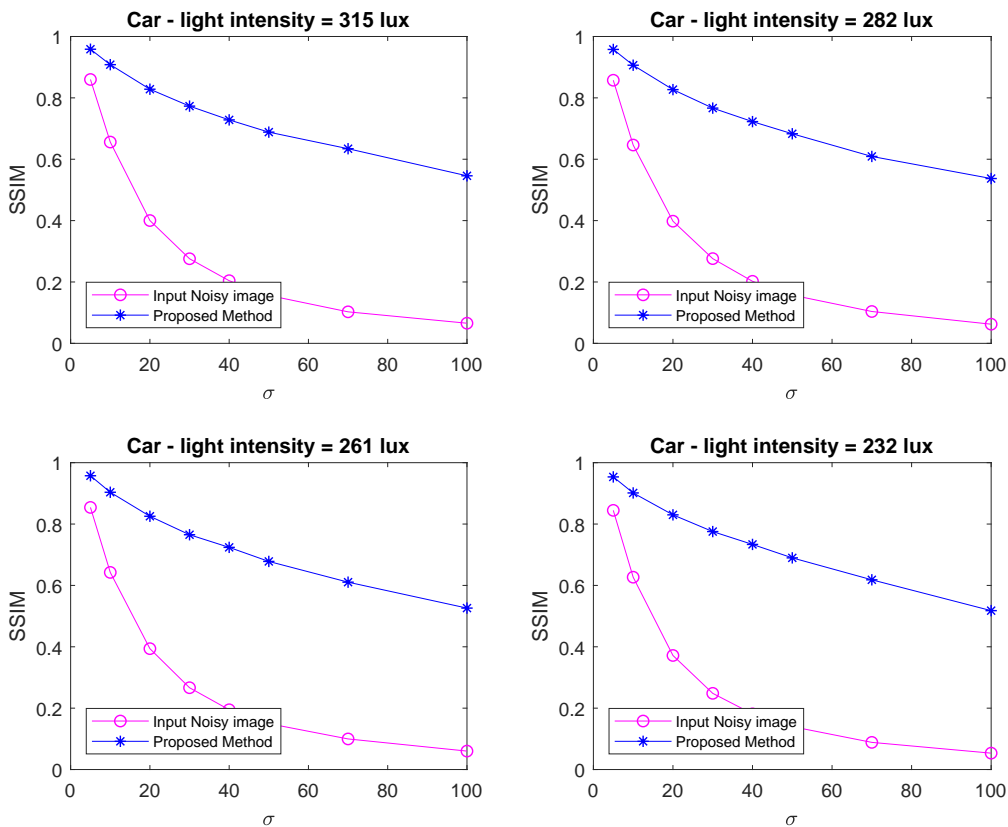


Fig. 13: Plot of SSIM values for Car images of different intensities against varying noise levels.

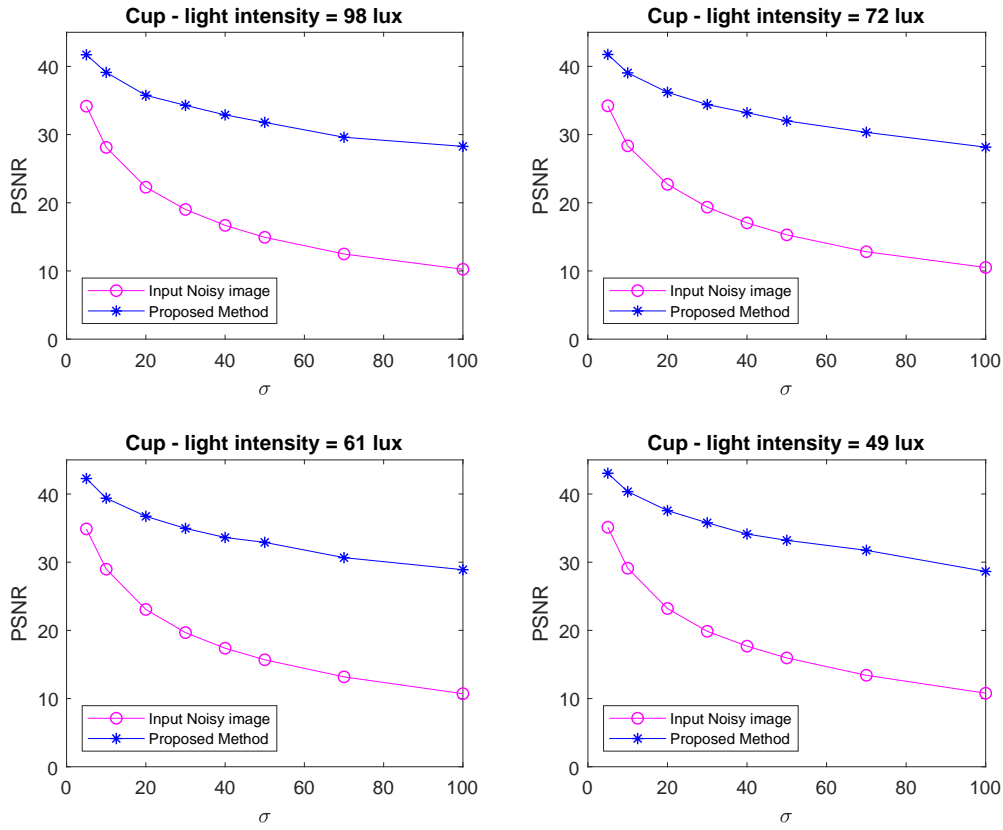


Fig. 14: Plot of PSNR values for Cup images of different intensities against varying noise levels.

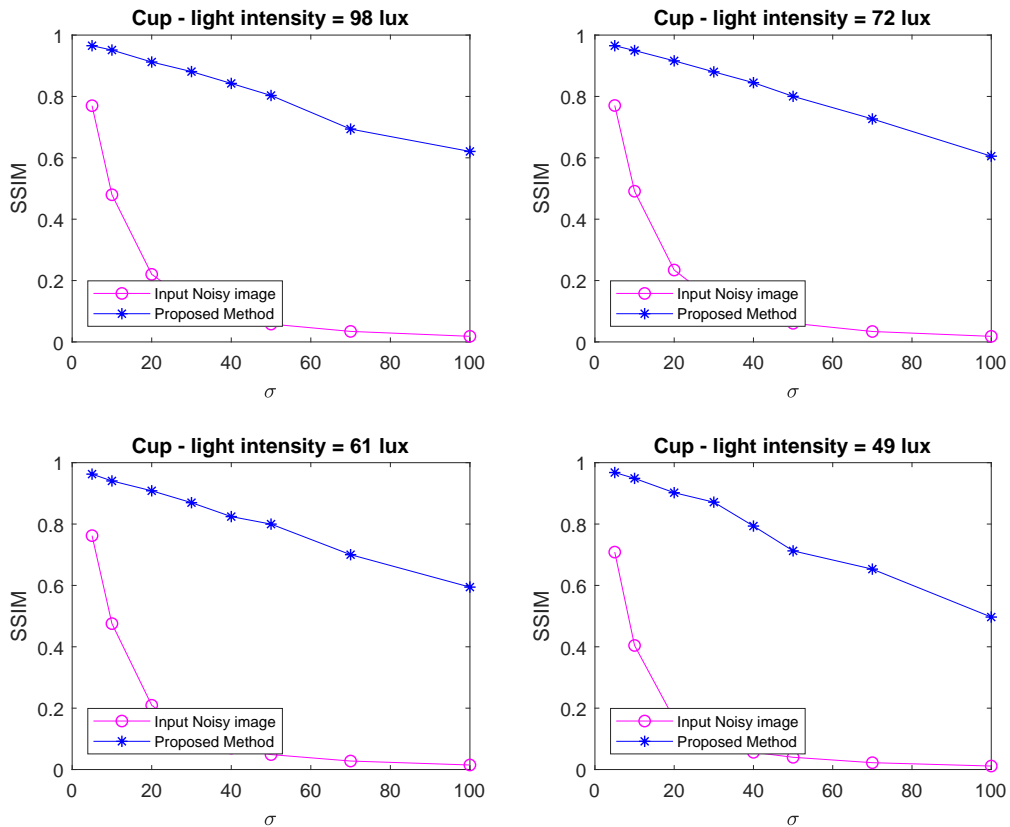


Fig. 15: Plot of SSIM values for Cup images of different intensities against varying noise levels.

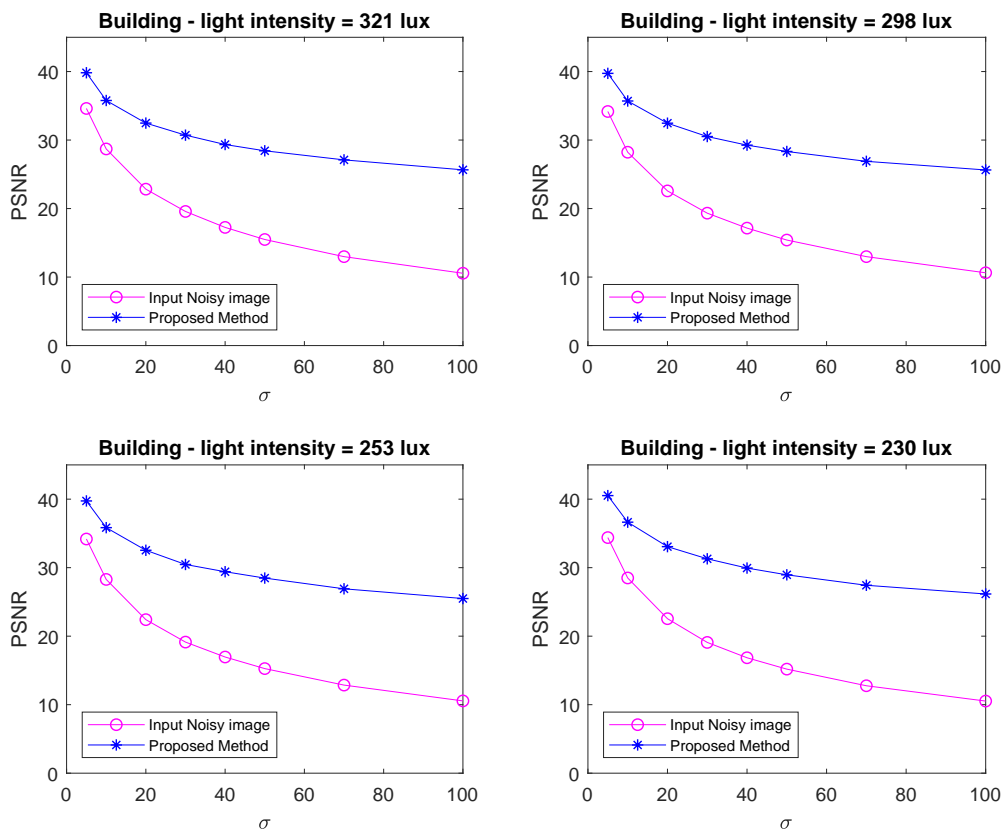


Fig. 16: Plot of PSNR values for Building images of different intensities against varying noise levels.

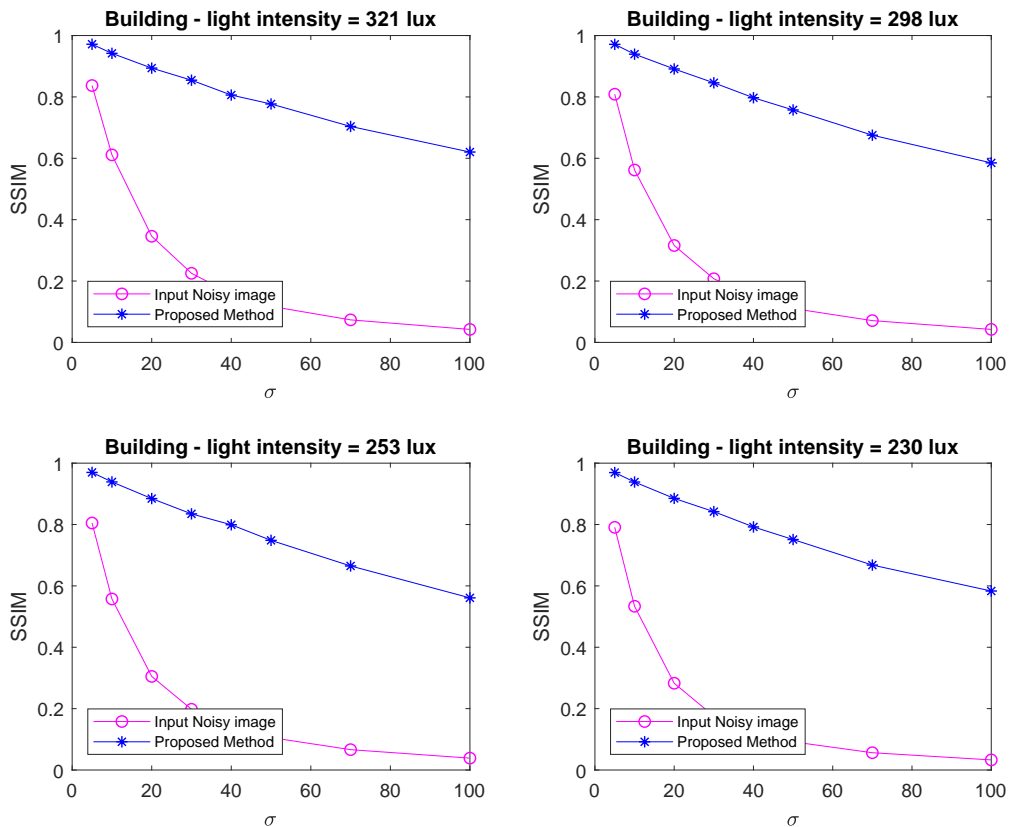


Fig. 17: Plot of SSIM values for Building images of different intensities against varying noise levels.

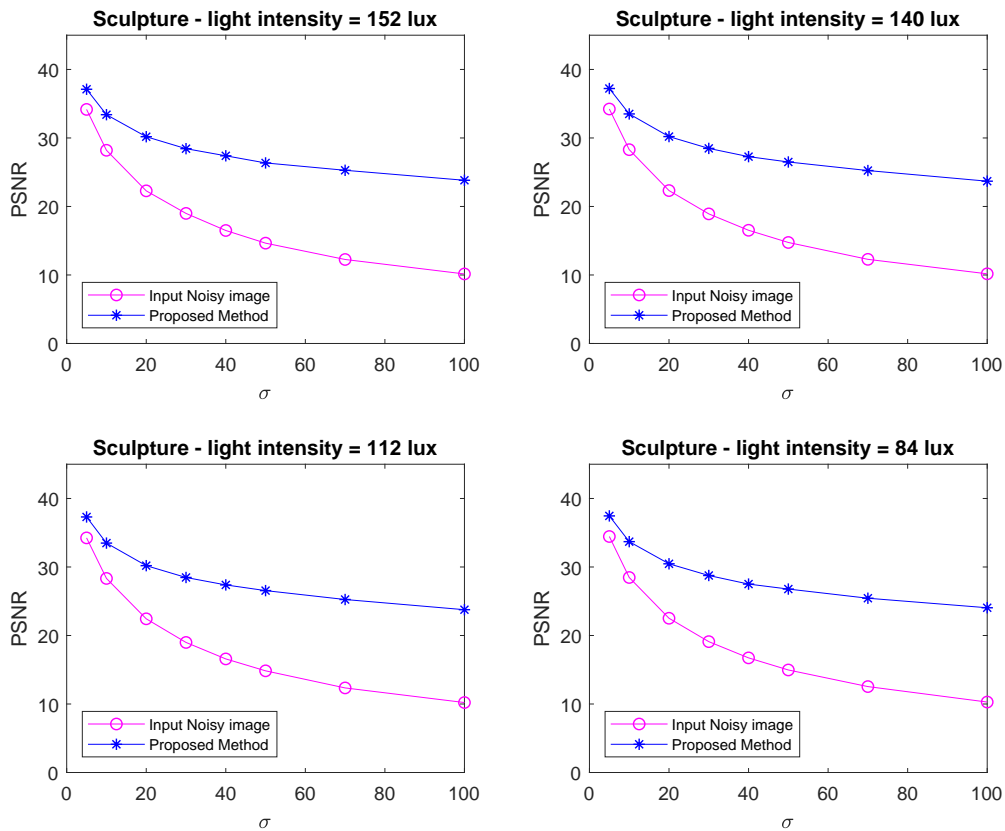


Fig. 18: Plot of PSNR values for Sculpture images of different intensities against varying noise levels

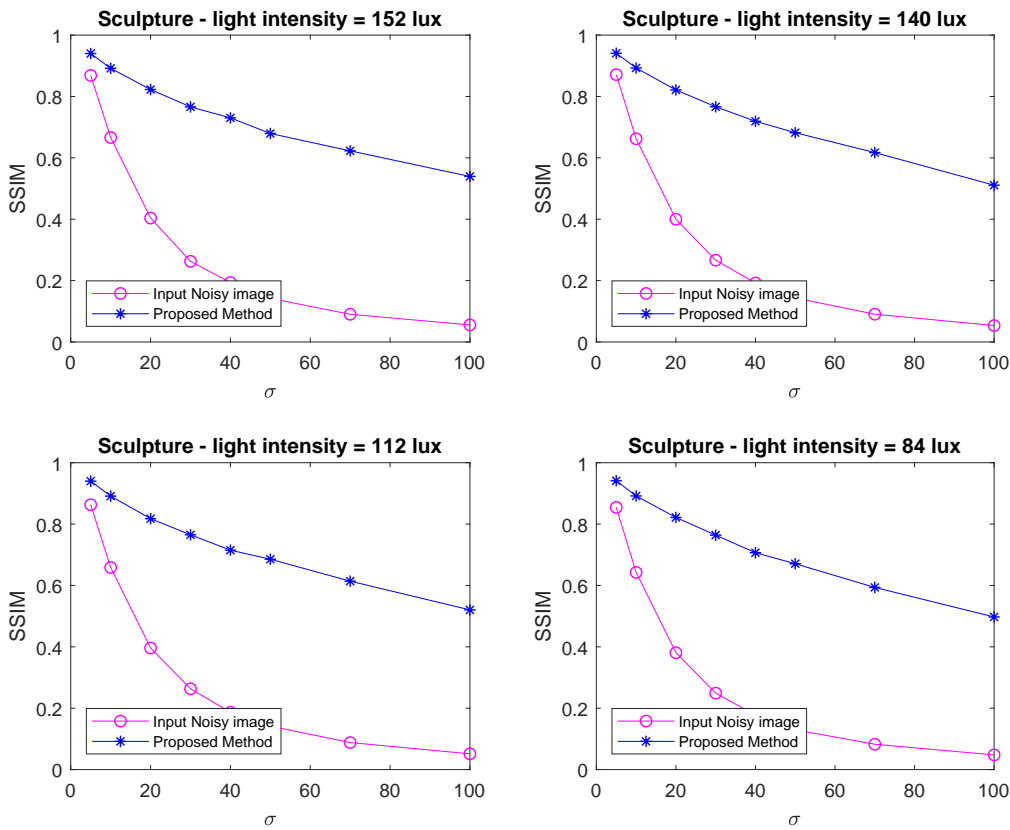
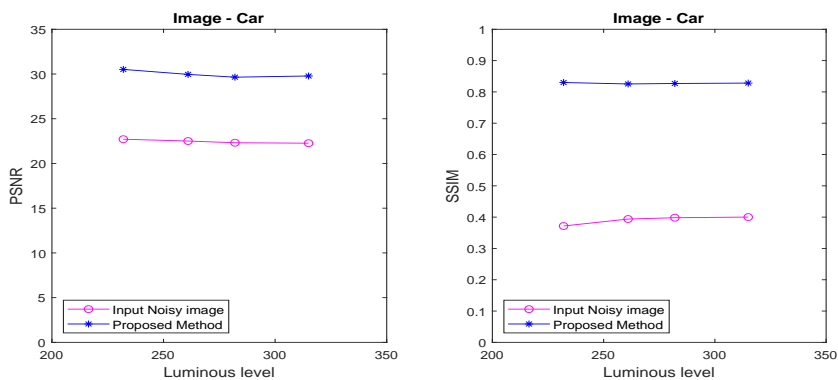
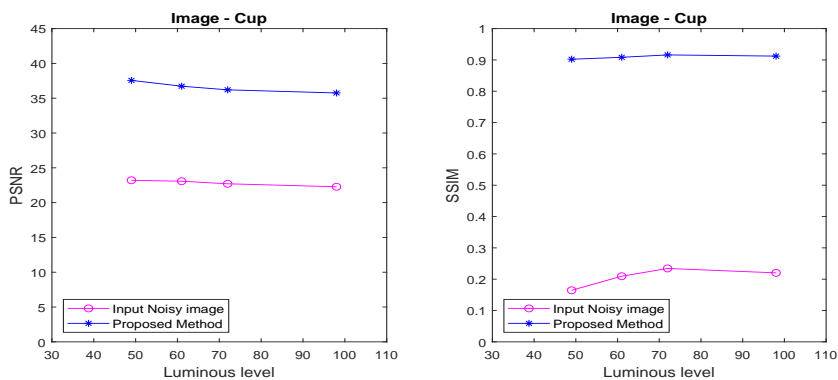


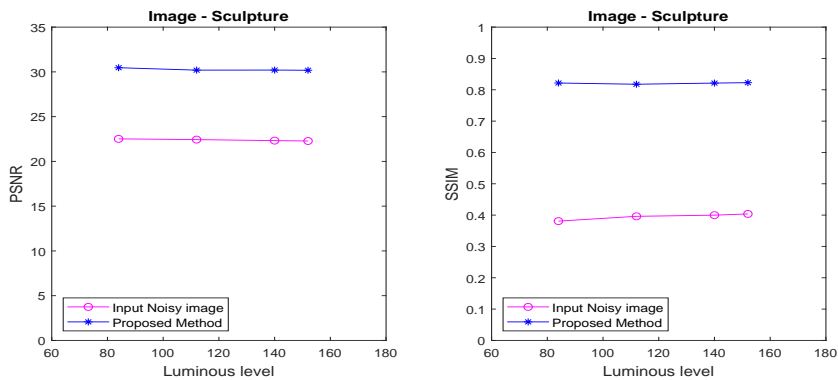
Fig. 19: Plot of SSIM values for Sculpture images of different intensities against varying noise levels.



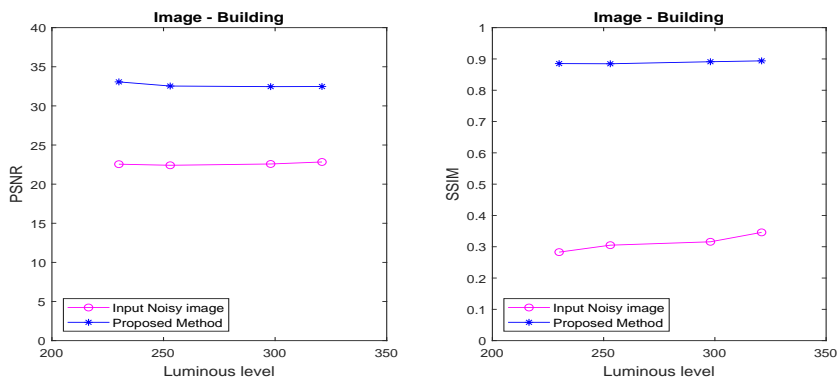
(a) Car image



(b) Cup image



(c) Sculpture image



(d) Building image

Fig. 20: Plot of quality metrics for the images against different luminous levels.

From the tables and graphs, it is evident that the performance of the proposed method in terms of quality metrics like PSNR and SSIM is far better than that of image denoising based on wavelet thresholding which uses wavelet transforms. The graphs reveal that as the noise level values increase, the proposed method's performance improvement relatively increases. In other words, the PSNR and SSIM values of the proposed method are very high compared to the PSNR and SSIM values of the noisy image at higher noise levels than at the lower noise levels. From figure (20), it is evident that the performance of the proposed method is stable and consistent at any light intensity level when used on low light images

VI. CONCLUSION

A noise removal method for the images with low luminous levels in sparse domain with the help of GMM is implemented in this paper. The sparse representation of the image is obtained by transforming the image into the wavelet domain. The simulation was done on standard test images and low luminous level images created for this work. Quality metrics values calculated show that the proposed technique effectively denoises images by retaining the structural similarity. Simulation performed on low luminous level natural images with different intensities shows that the method is efficient in denoising the images taken at different light intensities. Future work can be done to incorporate a method to improve the resolution of the output image.

REFERENCES

- [1] Anandbabu,Gopatoti, Image Denoising using spatial filters and Image Transforms: A Review, *International Journal for Research in Applied Science and Engineering Technology*, 6, 3447-3452, 2018, 10.22214/ijraset.2018.4571.
- [2] Cai N, Zhou Y, Wang S et al., Image denoising via patch-based adaptive Gaussian mixture prior method, *SIVIP*, 2016.
- [3] Jean-LucStarck, E J Candes, D L Donoho, The curvelet transform for image denoising, *IEEE Transactions on Image Processing*, vol. 11, no. 6, pp.670-684,2002.
- [4] Julie Delon, Antoine Houdard, Gaussian Priors for Image denoising, Bertalmo, Marcelo, *Denoising of Photographic Images and Video: Fundamentals*, Open Challenges and New Trends, 978-3- 319-96029-6, fihal-01800758f,(2018).
- [5] Chunli Wang, ChunleiZhang, PengtuZhang, (2012), Denoising algorithm based on wavelet adaptive threshold, *Physics Procedia*, 24, 678685.
- [6] LiuYali, Image Denoising Method based on Threshold, Wavelet Transform and Genetic Algorithm, *International Journal of Signal Processing, Image Processing and Pattern Recognition*, 8, 29-40, (2015).
- [7] Wang, Ronghao, et al.,(2015), A New Wavelet Thresholding Function Based on Hyperbolic Tangent Function, *Mathematical Problems in Engineering*, 10.1155/2015/528656.
- [8] Patil, Rajesh. (2015). Noise Reduction using Wavelet Transform and Singular Vector Decomposition.*Procedia Computer Science*, 54. 849-853. 10.1016 /j.procs.2015.06.099.
- [9] Luis Cadena, Darwin Castillo, AleksandrZotin, Franklin Cadena, Patricia Diaz, Evaluation of Noise Reduction Filters in Medical Image Processing using OpenMP, *IAENG International Journal of Computer Science*, vol. 46, no.4, pp582-593, 2019
- [10] Luis Cadena, Alexander Zotin, Franklin Cadena, Anna Korneeva, Alexander Legalov, Byron Morales, Noise Reduction Techniques for Processing of Medical Images, *Lecture Notes in Engineering and Computer Science: Proceedings of The World Congress on Engineering*, 2017, 5-7 July, 2017, London, U.K., pp496-500
- [11] Jing-yi Lu, Hong Lin, Dong Ye, Yan-shengZhang, A New Wavelet Threshold Function and Denoising Application, *Mathematical Problems in Engineering*, 2016, 1-8, 10.1155/2016/3195492.
- [12] Liu, Yali, Image Denoising Method based on Threshold, Wavelet Transform and Genetic Algorithm, *International Journal of Signal Processing, Image Processing and Pattern Recognition*, 8, 29-40, 2015,10.14257/ijcip.2015.8.2.04.
- [13] E Luo, S H Cha, T Q Nguyen, , Adaptive Image Denoising by Mixture Adaptation, *IEEE Transactions on Image Processing*, vol. 25, no. 10, Oct. pp.4489-4503, 2016.
- [14] Martin D, Fowlkes C, Tal D, Malik J, A database of human segmented natural images and its application to evaluating segmentation algorithms and measuring ecological statistics, *8th international conference on computer vision, ICCV*, vol. 2, pp.416-423, 2001.
- [15] Yu-Feng Li, Image denoising based on undecimated discrete wavelet transform, *International Conference on Wavelet Analysis and Pattern Recognition*, Beijing, pp.527-531, 2007.
- [16] S. Strano, M. Terzo, An Unscented Kalman Filter for Nonlinear Hysteretic System Identification with State Constraints and Adaptation of Measurement Noise Covariance, *Lecture Notes in Engineering and Computer Science: Proceedings of The World Congress on Engineering*, 2017, 5-7 July, 2017, London, U.K., pp716-721
- [17] Luis Cadena, Darwin Castillo, AleksandrZotin, Patricia Diaz, Franklin Cadena, Gustavo Cadena, and Yuliana Jimenez, Processing MRI Brain Image using OpenMP and Fast Filters for Noise Reduction, *Lecture Notes in Engineering and Computer Science: Proceedings of The World Congress on Engineering and Computer Science*, 2019, 22-24 October, 2019, San Francisco, USA, pp499-504
- [18] XueGuo, FengLiu, Yiting Chen, and XuetaoTian, Warm Start of Multi-channel Weighted Nuclear Norm Minimization for Color Image Denoising, *IAENG International Journal of Computer Science*, vol. 46, no.4, pp575-581, 2019

Sreekala K. is pursuing PhD in the field of Signal and Image processing from Visvesvaraya Technological University, Belagvi. She has completed Bachelors degree in Electronics and Communication Engineering from Visvesvaraya Technological University, Belagvi, and Masters degree in Electronics from Anna University Chennai, with more than 10 years of experience in both academics and industry. She has published papers in international conferences and journals. Her area of interest is Computer Vision and Image Processing.

SateeshKumar H.C. is Professor and Head, Department of Electronics and Communication Engineering, Saphagiri College of Engineering, Bengaluru. He obtained B.E. degree in Electronics Engineering from Bangalore University and his specialization in Master degree was Bio-Medical Instrumentation from Mysore University. He obtained his Ph. D degree in the area of Image Processing from Bangalore University. He has over 35 research publications in refereed International Journals and Conference Proceedings. His area of interest is in the field of Signal Processing and Communication Engineering.

Raja K. B. is Professor and Chairman, Department of Electronics and Communication Engineering, University Visvesvaraya College of Engineering, Bangalore University, Bengaluru. He obtained his B.E. and M.E. in Electronics and Communication Engineering from University Visvesvaraya College of Engineering, Bengaluru. He was awarded Ph.D. in Computer Science and Engineering from Bangalore University. He has over 200 research publications in refereed International Journals and Conference Proceedings. His research interests include Image Processing, Biometrics, VLSI Signal Processing, and Computer Networks.